JMI
Jurnal Multidisiplin Indonesia

Volume 4 Number 7 July, 2025
E-ISSN: 2964-9048 | P-ISSN: 2963-2900
https://jmi.rivierapublishing.id/index.php/rp

Comparative Analysis Of Flexible Pavement Damage Models Between Mdpj 2024 And Asphalt Institute And Aashto Mepdg

Kevin Briant Pasaribu[1*], Taqia Rahman[2], Latif Budi Suparma[3]
[1,2,3] Universitas Gadjah Madan, Indonesia
Email : kevinbriantpasaribu@mail.ugm.ac.id[1*] taqia.rahman@ugm.ac.id[2],
lbsuparma@ugm.ac.id[3]

Abstract

Reliable road infrastructure is crucial for the economy. However, high traffic loads can accelerate damage to flexible pavements, primarily fatigue cracking and permanent deformation (rutting). This study evaluates the performance of pavement structures designed according to the Indonesian Pavement Design Manual (MDPJ) 2024 by comparing its damage predictions against international methods, namely the Asphalt Institute and AASHTO MEPDG, across various road classifications. Through mechanistic simulation using KENPAVE, the resulting strain values were used as input to predict the number of allowable load repetitions (ESAL) until failure occurs. The results show that all three methods consistently identify fatigue cracking as the critical damage type that occurs before rutting. However, there are significant differences in the magnitude of the predicted ESAL values. The Asphalt Institute method is the most conservative, producing the lowest fatigue cracking ESAL, while AASHTO MEPDG predictions are closer to, yet still lower than, the most optimistic predictions of MDPJ 2024. Therefore, this study concludes that further calibration of the MDPJ 2024 model with actual field data is essential to improve the accuracy of service life predictions for pavements in Indonesia.

Keywords : Flexible Pavement, MDPJ 2024, Asphalt Institute, AASHTO MEPDG, Fatigue Cracking and Rutting

Corresponding Author; Kevin Briant Pasaribu
Email: kevinbriantpasaribu@mail.ugm.ac.id

INTRODUCTION

Highways provide various benefits, such as driving economic growth, improving connectivity, which plays a role in security and political aspects, and facilitating mobility between regions. However, behind these various advantages, high traffic volumes accelerate the rate of wear and damage to road pavements. The link between traffic intensity and the level of pavement deterioration has been widely demonstrated, with heavy traffic requiring more frequent maintenance and rehabilitation. (Almeida et al., 2021) . Furthermore, heavy vehicles , especially those carrying excessive loads, overload flexible pavement and accelerate the deterioration process. Research shows that overloading vehicles can reduce pavement service life by up to 50%. (Jihanny, 2021) .

Flexible pavement, also known as asphalt pavement, is constructed from several layers with varying roles and material types. This pavement structure consists of key elements that support each other to distribute loads efficiently. This type of pavement consists of several layers, including the asphalt layer on top (*surface course*) , the upper foundation layer (base *course*), the lower foundation (*subbase*), and the base soil layer

(*subgrade*). (Wayne et al., 2011) . The main characteristic of flexible pavement is the load applied by the wheels transmitted through layers of pavement, where each layer functions to spread the load over a wider area, thereby reducing pressure on the subgrade (*subgrade*). (VenkatCharyulu & Viswanadh, 2021) . The application of flexible pavements to highways offers several advantages . Flexible pavements typically require lower initial construction costs than rigid pavements, making them a more cost-effective solution for various road projects. (Skrzypczak et al., 2018) .

and causes of damage to flexible pavements include fatigue cracking *and* permanent deformation (*rutting*). Fatigue cracking *generally appears* due to repeated traffic loads that trigger the formation of small cracks in the pavement, which over time grow and merge into large cracks (Hafeez et al., 2013) . Meanwhile, permanent deformation (*rutting*) occurs on the wheel track due to a combination of high temperatures and large vehicle load pressure, which ultimately causes deformation to form in the form of depressions on the road surface. (Hussan et al., 2019) . These two types of damage are often associated with inappropriate pavement structure design, inadequate material quality, and environmental conditions such as high temperatures and poor drainage. A thorough understanding of the mechanisms of fatigue cracking *and* permanent deformation (*rutting*) is essential as a basis for planning, maintaining, and rehabilitating flexible pavements in order to extend the service life of roads. This study analyzes the performance of flexible pavement designs in the 2024 MDPJ to predict and control two main damages, namely fatigue cracking and *permanent* deformation (*rutting*). The goal is to extend the service life of roads with appropriate design guidelines.

This study evaluates the performance of flexible pavement structural design in the Road Pavement Design Manual (MDPJ) 2024 by comparing it to the damage models in the Road Pavement Design Manual (MDPJ) 2024, Asphalt Institute, and AASHTO MEPDG, as well as analysis using KENPAVE software. The evaluation focuses on predicting two main damages, namely fatigue cracking *and* permanent deformation (*rutting*), by comparing the results of the permitted load repetition number (ESAL) predictions on various road classifications. The results of this study are expected to provide a comprehensive overview and useful technical input for the pavement design and evaluation process in Indonesia.

RESEARCH METHODS

Study This study uses a descriptive quantitative research method through software simulation. The research is *hypothetical* by analyzing technical data obtained from the 2024 Road Pavement Design Manual in the form of flexible asphalt pavement design data with aggregate foundation layers (Small Roads, Medium Roads, Highways, and Toll Roads), material characterization data consisting of elastic modulus and *Poisson's ratio*, and loading data on pavement structures to anticipate future pavement design problems.

Simulation of flexible pavement structure response was carried out using KENPAVE software (KENLAYER module) to obtain tensile strain (*horizontal strain*) and compressive strain (*vertical strain*) values. This strain data is then analyzed using the

transfer function (*transfer function) based on three design guidelines, namely MDPJ 2024, Asphalt Institute, and AASHTO MEPDG to predict the number of permitted load repetitions* (ESAL) allowed before fatigue cracking *and* permanent deformation (*rutting*) occur.

Flexible Pavement Design Data

In this study, the road pavement structure was modeled based on four types of road classification according to the 2024 Road Pavement Design Manual (MDPJ) standards, namely FFF (1) 2 (Small Road), FFF (1) 5 (Medium Road), FFF (1) 7 (Highway), and FFF (1) 9 (Toll Road) using a lower foundation layer in the form of an aggregate base. Each type of road has different pavement structure design characteristics, adjusted to the level of traffic volume and the need for bearing capacity. Design data for flexible asphalt pavement with an aggregate base layer for FFF (1) 2 (Small Roads), FFF (1) 5 (Medium Roads), FFF (1) 7 (Highways), and FFF (1) 9 (Toll Roads) can be seen in Table 1, Table 2, Table 3, and Table 4.

Table 1. Small Road Pavement Thickness Data

FFF (1) 2 (Small Road)	
Pavement Thickness (mm)	
Toilet AC	40
AC BC	65
	80
Class A Aggregate Foundation Layer	200
Class B Aggregate Foundation Layer	150

Source: Ministry of Public Works and Public Housing, 2024

Table 2. Medium Road Pavement Thickness Data

FFF (1) 5 (Moderate Road)	
Pavement Thickness (mm)	
Toilet AC	40
AC BC	60
AC *Base*	80
	80
Class A Aggregate Foundation Layer	200
Class B Aggregate Foundation Layer	150
Coarse Grained Selected Embankment or LFA Class C or Cement Stabilization	200

Source: Ministry of Public Works and Public Housing, 2024

Table 3. Highway Pavement Thickness Data

FFF (1) 7 (Highway)	
Pavement Thickness (mm)	
Toilet AC	40
AC BC	75
AC *Base*	100
	100
Class A Aggregate Foundation Layer	200
Class B Aggregate Foundation Layer	150
Coarse Grained Selected Embankment or LFA Class C or Cement Stabilization	200

Source: Ministry of Public Works and Public Housing, 2024

Table 4. Toll Road Pavement Thickness Data

FFF (1) 9 (Toll Road)	
Pavement Thickness (mm)	
Toilet AC	40
AC BC	60
AC *Base*	80
	80
	90
Class A Aggregate Foundation Layer	200
Class B Aggregate Foundation Layer	150
Coarse Grained Selected Embankment or LFA Class C or Cement Stabilization	200

Source: Ministry of Public Works and Public Housing, 2024

Material Characterization Data

In the flexible pavement structure analysis process in this study, the modulus of elasticity and *Poisson's ratio are required* for each material layer. Based on MDPJ 2024, all pavement layers have a modulus of elasticity and *Poisson's ratio value* . This value is used in analyzing the tensile strain (*horizontal strain*) and compressive strain (*vertical strain*) values using KENPAVE software with the KENLAYER module. Material characterization data consisting of the modulus of elasticity and Poisson's ratio based on the 2024 Road Pavement Design Manual can be seen in Table 5.

Table 5. Material Characterization

Material	Modulus E (MPa)	*Poisson's* ratio	Degree of Anisotropic (n)	Vb	K	Shear Modulus, f (MPa)
Toilet AC	1,100	0.40	1	12.2	0.0064070	-
AC BC	1,200	0.40	1	11.5	0.0058865	-
AC *Base*	1,500	0.40	1	11.5	0.0054321	-
LFA Sub Layer 1	220	0.35	2	-	-	163.0
LFA Sub Layer 2	170	0.35	2	-	-	125.7
LFA Sub Layer 3	131	0.35	2	-	-	96.9
LFA Sub Layer 4	101	0.35	2	-	-	74.7
LFA Sub Layer 5	78	0.35	2	-	-	57.6
Basic Land	60	0.45	2	-	-	41.4

Source: Ministry of Public Works and Public Housing, 2024

Loading Data

The pavement loading in this study was modeled using *single axle dual tires* (SADT). *The single axle dual tires* (SADT) model was chosen because it complies with the Road Pavement Design Manual (MDPJ 2024) standards, where traffic loading is generally simplified to a single axle load with dual wheels. This approach allows for the calculation of stresses, strains, and deflections in each pavement layer to be analyzed more representative of real traffic conditions. The traffic load is assumed to originate

from an 80 kN vehicle axle, consisting of two pairs of dual wheels. Each wheel transmits a load of 20 kN to the road surface. The wheel contact area with the road surface is assumed to be circular with a pressure of 750 kPa, resulting in a contact radius of 110 mm. The distance between the wheels on one side of the axle (*dual wheel spacing*) is 330 mm, while the distance between the left and right axle sides is 1800 mm. Loading data obtained from the 2024 Road Pavement Design Manual can be seen in Figure 1 and Table 6.

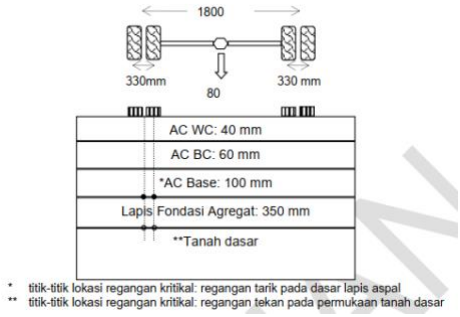

Figure 1. Loading on Pavement Structure

(Source: Ministry of Public Works and Public Housing, 2024)

Table 6. Loading Data on Pavement Structures

***Single Axle Dual Tires* (SADT)**	
Load Type	Double Wheel
Contact Pressure	750 kPa
Contact Radius	11 cm
Wheelbase	33 cm

Source: Ministry of Public Works and Public Housing, 2024

KENLAYER Method Procedure

In this study, the KENLAYER method on KENPAVE is used to analyze the response of road pavement structures in a *linear elastic* layered manner to obtain tensile strain (*horizontal strain*) and compressive strain (*vertical strain*) values using a mechanistic-empirical approach. The procedure for using the KENLAYER method is carried out through several stages, namely LAYERINP, *General*, *Zcoord*, *Layer, Moduli*, and *Load*. After all stages have been carried out and *the file* has been saved, the next step is to return to the KENPAVE main menu and after that the *running process* is carried out through the KENLAYER menu. To see the results of the tensile strain analysis (*horizontal strain*) and compressive strain (*vertical strain*), you can open the *file menu* through the *Editor menu.*

Damage Models in MDPJ 2024, Asphalt Institute, and AASHTO MEPDG

In this study, the damage model is used to predict the ability of flexible pavement structures to withstand traffic loads before failure in the form of fatigue cracking and permanent deformation (rutting) occurs. The *horizontal tensile strain* and vertical compressive strain *values* obtained based on the KENLAYER method on KENPAVE are then used as input in the fatigue cracking (Nf) and permanent deformation (rutting) (Nd)

formula equations *in* the *Road* Pavement Design Manual (MDPJ) 2024, Asphalt Institute, and AASHTO Mechanistic-Empirical Pavement Design Guide (AASHTO MEPDG) to obtain the maximum permissible load repetition (ESAL) value that can be supported by the pavement structure based on the Road Pavement Design Manual (MDPJ) 2024 before fatigue cracking *and* permanent deformation (*rutting*) occur.

A. *Fatigue Cracking* and Rutting *Damage* Models in MDPJ 2024

In medium to heavy load pavements using conventional asphalt, the transfer function describes the relationship between the maximum tensile strain due to a load and the number of load repetitions that can still be tolerated to measure performance against fatigue cracking *(* Ministry of Public Works and Public Housing, 2024). The closer to the surface of the pavement, the elastic strain tends to increase. Therefore, by limiting the elastic compressive strain at the subgrade surface, the elastic compressive strain in the layers above it can also be controlled, so that the overall accumulation of plastic strain can be maintained (Ministry of Public Works and Public Housing, 2024). The fatigue cracking and permanent deformation (rutting) damage models *in* the *2024* Road Pavement Design Manual (MDPJ) can be seen in Equation 1 and Equation 2.

$$\boldsymbol{N = \frac{SF}{RF} \times \left[\frac{6918 \times (0{,}856 V_b + 1{,}08)}{E_{mix}^{0{,}36} \times \mu\varepsilon}\right]^5} \quad (1)$$

with,

N : Number of repetitions of load permit
με : Tensile strain due to load (*microstrain*)
V_b : Volume of asphalt in the mixture (%)
E_{mix} : Modulus of asphalt mixture (MPa)
SF : *Shift factor* between laboratory test results and *in-service fatigue lives* (value presumptive = 6)
RF : Reliability factor at 90% is 3.9

$$N = \left[\frac{9300}{\mu\varepsilon}\right]^7 \quad (2)$$

with,

N : Number of repetitions of load permit
με : Compressive strain at the base soil surface (*microstrain*)

B. *Fatigue Cracking* and Rutting *Damage* Models at the Asphalt Institute

Road damage can be triggered by various causes, and one of the main factors is overloading, where the load on each axle of the vehicle exceeds the specified standard limit (Hadiwardoyo et al., 2012). The type of *fatigue cracking damage* is analyzed based on the horizontal tensile strain value that occurs at the bottom of the asphalt surface layer due to traffic loads on the pavement. Meanwhile, *rutting* damage is evaluated from the compressive strain that appears at the top of the subgrade or just below the lower foundation layer. Based on these two types of damage, the number of load repetitions that cause damage can be calculated, namely Nf (for *fatigue*) and Nd (for *rutting*), by referring to the tensile strain value below the surface layer and the compressive strain

above the subgrade or below the lower foundation. One approach used for this calculation is through the equation from the Asphalt Institute Method (Simanjuntak, 2014). The *fatigue* cracking equation for flexible pavement is used to determine the number of load repetitions that can be sustained, based on the horizontal tensile strain (Ɛt) beneath the pavement surface layer (Asphalt Institute, 1982). The fatigue cracking damage model equation *at* the Asphalt Institute can be seen in Equation 3.

$$Nf = 0{,}0796 \times (\varepsilon_t)^{-3{,}291} \times (E)^{-0{,}854} \quad (3)$$

with,

Nf : Number of repetitions of *fatigue cracking load* .
Ɛt : Horizontal tensile strain at the bottom of the surface layer.
E : Modulus of elasticity of the surface layer.

The equation for permanent deformation damage (*rutting*) is used to calculate the number of load repetitions that can be supported, based on the vertical compressive strain that occurs at the top of the subgrade surface (Asphalt Institute, 1982). The equation for the permanent deformation damage (*rutting*) model at the Asphalt Institute can be seen in Equation 4.

$$Nd = 1{,}365 \times 10^{-9} \times (\varepsilon_c)^{-4{,}477} \quad (4)$$

with,

Nd : Number of repetitions of *rutting load* .
Ɛc : Vertical compressive strain at the top of the subgrade layer.

C. *Fatigue Cracking* and Rutting *Damage* Models in AASHTO MEPDG

In AASHTO MEPDG, the two main damage modes focused on flexible pavements are *fatigue cracking* and *rutting* . *Fatigue cracking* is predicted based on the accumulation of horizontal tensile strains at the base of the asphalt layer, which causes microcracking and develops into macrocracking as the load cycles increase (Bennet et al., 2014). *Rutting* is calculated from the accumulation of vertical compressive strains in the subgrade and sub-base layers, which cause permanent deformation (Ceylan et al., 2009). The prediction method in AASHTO MEPDG uses a damage transfer model (*transfer functions*) that relates the number of allowable load repetitions to material, traffic, and climate parameters. This analysis is performed iteratively to project pavement performance throughout the design life, taking into account reliability factors and input variability (Li et al., 2016). The *fatigue cracking equation* for flexible pavements is used to determine the number of load repetitions that can be supported, based on the horizontal tensile strains below the pavement surface layer (AASHTO, 2008). *The fatigue cracking* damage model equation in AASHTO MEPDG can be seen in Equation 5.

$$N_{f-HMA} = k_{f1}(C)(C_h)\beta_{f1}(\varepsilon_t)^{k_{f2}\beta_{f2}}(E)^{k_{f3}\beta_{f3}} \quad (5)$$

with,

$N_{f\text{-}HMA}$: The number of axle loads permitted on flexible pavement until fatigue cracking *occurs* .
ε_t : Tensile strain at critical location .
E : The dynamic tensile strength measured in compression is used based on the results of a previous study by Rupiani et al. (2023) of 4845.39 Mpa or 702764.404 psi.
K_{f1} , K_{f2} , K_{f3} : Global field calibration parameters (based on NCHRP 1-40D *Recalibration* , with values of K_{f1} = 0.007566, K_{f2} = –3.9492, K_{f3} = –1.281).

β_{f1} , β_{f2} , β_{f3} : Local or mixed field calibration factors; all these factors are set to 1.0 for global calibration.

C : K constant which depends on the properties of the mixture and is calculated using Equation 6 and Equation 7.

$$C = 10^{M} \quad (6)$$

$$M = 4{,}84\left(\frac{V_{be}}{V_a + V_{be}} - 0{,}69\right) \quad (7)$$

with,

V_a : Air cavity when the road is opened to traffic (%).

V_{be} : Effective asphalt content based on the volume of mixture installed on the road pavement (%).

C_h : F thickness correction factor, which is calculated using equation 8.

$$M = \frac{1}{0{,}000398 + \frac{0{,}003602}{1 + e^{(11{,}02 - 3{,}49 \times h_{HMA})}}} \quad (8)$$

rutting damage is used to calculate the number of load repetitions that can be supported, based on the vertical compressive strain that occurs at the top of the subgrade surface (AASHTO, 2008). The equation for the permanent deformation damage model (*rutting*) in AASHTO MEPDG can be seen in Equation 9.

$$N = \left(\frac{\rho}{-\mathrm{Ln}\left(\frac{\Delta_{psoil}}{h_{soil} \times \beta_{s1} k_1 \times \varepsilon_v \times \left(\frac{\varepsilon_o}{\varepsilon_r}\right)} \right)} \right)^{\frac{1}{\beta}} \quad (9)$$

with,

N : Number of repetitions of *rutting load* .

Δ_{psoil} : The value (Δ_{psoil} : 0.79 inch) in this study adopts the *rutting failure criteria* according to the Indian Roads Congress IRC 37:2018, which defines failure as occurring when the average rutting depth exceeds 20 mm (Banerjee et al., 2024).

h_{soil} : Austroads (2017) recommends a depth of 1 m for the weak layer below *the subgrade (Section 5.3.7), so in this study an Hsoil value of 1000 mm was used. Therefore, in this study an* $h_{soil\ value}$ of 39.4 inches was used .

k_1 : Global calibration coefficient; k_1 = 2.03 for granular materials , and k_1 = 1.35 for fine-grained *materials* .

β_{s1} : Local calibration factor; this factor is set to 1.0 for global calibration; also called β_{GB} for unbound *base layers* and β_{SG} for subgrade *layers* .

ε_v : The average elastic or resilient vertical strain in the layer (inch/inch) calculated by the structural response model .

ε_o : Strain intercept (inch/inch) determined from repeated load laboratory tests against permanent deformation.

ε_r : Resilient (recoverable) strain (inch/inch) given in a laboratory test to obtain the material properties .

$\varepsilon_o / \varepsilon_r$: The value ($\varepsilon_o / \varepsilon_r$: 20.7) in this study was used based on the results of a previous study by Rupiani et al. (2023).

β and ρ : The values (β: 0.208) and (ρ: 2270.45) in this study were used based on the results of a previous study by Rupiani et al. (2023).

With this approach, the integration between the mechanistic analysis of KENPAVE and the empirical damage model from the 2024 Road Pavement Design Manual (MDPJ), Asphalt Institute, and AASHTO Mechanistic-Empirical Pavement Design Guide (AASHTO MEPDG) is expected to produce more accurate predictions regarding the durability of the 2024 MDPJ pavement structure based on the value of the number of load repetitions (ESAL) before fatigue cracking *and* permanent deformation (*rutting*) occur.

RESULTS AND DISCUSSION

Horizontal Strain and *Vertical Strain* Analysis using KENPAVE

Based on the analysis carried out on four road classifications based on the 2024 Road Pavement Design Manual (MDPJ), namely FFF(1) 2 (small roads), FFF(1) 5 (medium roads), FFF(1) 7 (highways), and FFF(1) 9 (toll roads) using KENPAVE software, the tensile strain (*horizontal strain*) and compressive strain (*vertical strain*) values were obtained for each road classification which can be seen in Table 7 and Figure 2.

Table 7. Summary of *Maximum Horizontal Strain* and *Maximum Vertical Strain Values*

Road Classification	*Maximum Horizontal Strain*	*Maximum Vertical Strain*
FFF (1) 2	0.0003238	0.0005397
FFF (1) 5	0.0002043	0.0002690
FFF (1) 7	0.0001612	0.0002242
FFF (1) 9	0.0001392	0.0002003

Source: Author, 2025

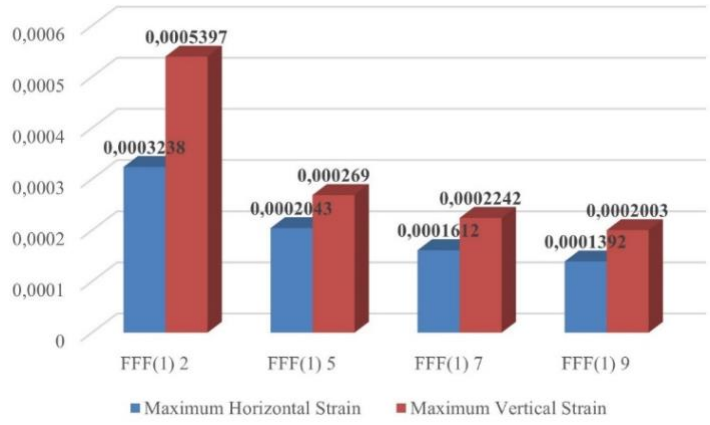

Figure 2. Comparison Graph *of Maximum Horizontal Strain* and *Maximum Vertical Strain*
(Source: Author, 2025)

The KENPAVE simulation results in Table 7 show a consistent downward trend in strain values as the road classification increases. The *maximum horizontal strain value* decreased from 0.0003238 at FFF(1) 2 (Minor Road) to 0.0001392 at FFF(1) 9 (Toll Road), or a decrease of 57%. Meanwhile, *the maximum vertical strain* decreased from 0.0005397 at FFF(1) 2 (Minor Road) to 0.0002003 at FFF(1) 9 (Toll Road), or a more significant decrease of 63%. This indicates that the pavement structure for higher road classifications is designed to have better stiffness and thickness. Smaller strains indicate a more effective load distribution through the pavement layers to the subgrade.

***Fatigue Cracking* and Rutting *Damage* Analysis Based on MDPJ 2024, AI, and AASHTO MEPDG**

output results from the KENPAVE program are in the form of maximum tensile strain values (*maximum horizontal strain*) and maximum compressive strain (*maximum vertical strain*) for each road classification. These values are then used to analyze the response of flexible pavement structures in predicting the number of repetitions of permissible load (ESAL) that can be supported by FFF(1) 2 (Minor Roads), FFF(1) 5 (Medium Roads), FFF(1) 7 (Highways), and FFF(1) 9 (Toll Roads) pavements against potential damage, especially fatigue cracking *and* permanent deformation (*rutting*) using the fatigue *cracking* and permanent deformation (*rutting*) damage model equations based on the Road Pavement Design Manual (MDPJ) 2024, Asphalt Institute, and AASHTO Mechanistic-Empirical Pavement Design using Equation 1, Equation 2, Equation 3, Equation 4, Equation 5, and Equation 9. Recapitulation of the number of repetitions of permissible load (ESAL) values obtained from the results of the analysis of fatigue cracking and permanent deformation (rutting) damage *on* four *road* classifications, based on the damage model approach between the Road Pavement Design Manual (MDPJ) 2024, Asphalt Institute, and AASHTO Mechanistic-Empirical Pavement Design shown in Table 8 and Figure 3.

Table 8. Summary of the Number of Repetitions of Load Permit (ESAL) Values

Road Classification	**MDPJ 2024**		**Asphalt Institute**		**AASHTO MEPDG**	
	Fatigue Cracking	Permanent Deformation (*Rutting*)	*Fatigue* Cracking	Permanent Deformation (*Rutting*)	*Fatigue* Cracking	Permanent Deformation (*Rutting*)
FFF(1) 2	3,054,833 ESAL	451 . 142 . 470 ESAL	156,304 ESAL	582 . 487 ESAL	2,566,794 ESAL	748,710,356,726 ESAL
FFF(1) 5	20,445,220 ESAL	59 . 035 . 694 . 933 ESAL	588,082 ESAL	13 . 156 . 237 ESAL	15,822,112 ESAL	493.700.210.977 ESAL
FFF(1) 7	66 . 851 . 081 ESAL	211 . 315 . 513 . 783 ESAL	1,282,605 ESAL	29 . 739 . 73 1 ESAL	40,332,048 ESAL	445,270,314,871 ESAL
FFF(1) 9	139 . 231 . 482 ESAL	465 . 172 . 459 . 90 3 ESAL	2,078,808 ESAL	49 . 261 . 433 ESAL	71,997,301 ESAL	418.170.345.878 ESAL

Source: Author, 2025

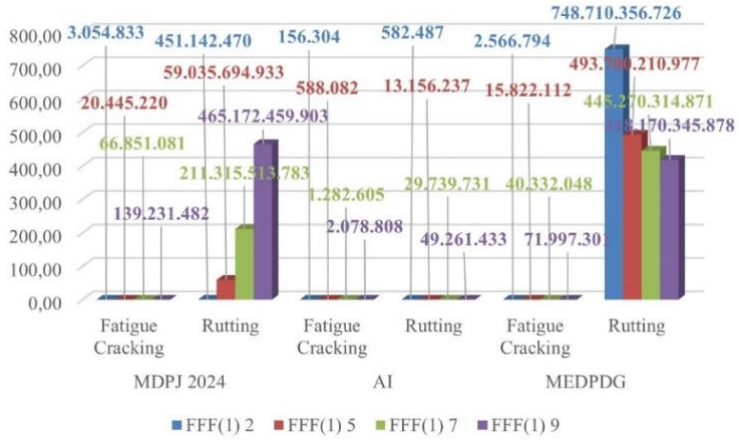

Figure 3. Graph of Allowable Load Repetition Count (ESAL) Values

(Source: Author, 2025)

Key Findings

Table 8 and the visualization in Figure 3 show variations in the number of repetitions of permissible load (ESAL) for two main types of damage in flexible pavement, namely fatigue cracking *and* permanent deformation (*rutting*) by comparing the damage model approach based on the Road Pavement Design Manual (MDPJ) 2024, Asphalt Institute, and AASHTO Mechanistic-Empirical Pavement Design. The three methods are consistent in predicting fatigue cracking *as* the main structural damage that occurs most quickly. To facilitate visual analysis, this comparison is presented in graphical form in Figure 4.

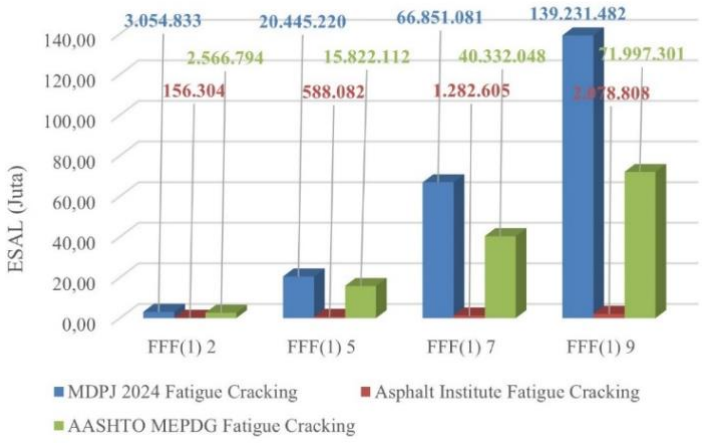

Figure 4. Comparison Graph of ESAL *Fatigue Cracking Values*

(Source: Author, 2025)

Based on the analysis results, pavement thicknesses designed using the 2024 Road Pavement Design Manual (MDPJ) yield significantly different ESAL values when evaluated using two international methods, namely the Asphalt Institute and AASHTO Mechanistic - Empirical Pavement Design. However, all three methods consistently agree

in predicting *fatigue* cracking as the dominant damage in all road classifications. The ESAL values for fatigue cracking *in* the 2024 MDPJ are consistently higher than those of the other two methods, namely the Asphalt Institute and AASHTO MEPDG for all road classifications. This indicates that the 2024 MDPJ is actually the most optimistic about fatigue cracking damage *compared* to the two international methods, because it produces consistently higher ESAL values for all road classifications. Meanwhile, for permanent deformation (*rutting*), the ESAL values of the 2024 MDPJ are always greater than those of the Asphalt Institute, indicating a higher level of optimism regarding this damage. However, when compared with AASHTO MEPDG, the ESAL value of MDPJ 2024 for permanent deformation (*rutting*) is smaller in FFF(1) 2 (Minor Roads), FFF(1) 5 (Medium Roads), and FFF(1) 7 (Highways), but is actually larger in FFF(1) 9 (Toll Roads). This condition raises the question of whether the pavement thickness design in MDPJ 2024 is optimal or *overdesigned , or whether the fatigue cracking* and permanent deformation (*rutting)* equation formulation in MDPJ 2024 has been well calibrated for field conditions in Indonesia.

On the other hand, the significant differences with the AASHTO MEPDG projections have raised questions about the feasibility of implementing this highly complex and highly detailed data-intensive method in Indonesia. The successful implementation of AASHTO MEPDG relies heavily on data availability and a comprehensive local calibration process. Without these, the accuracy and reliability of the predictions for Indonesian conditions are questionable.

Given that this research is still *hypothetical* and has not been tested with a direct case study, the results of this analysis are expected to provide a bridge for further research. Further research that tests the performance of pavements designed using the 2024 MDPJ using direct field *monitoring data* is urgently needed. The actual service life data and the types of damage that occur can then be used to validate the prediction accuracy of the three models, conduct intensive calibration of key parameters in each model, and determine which model is most representative or generate a conversion factor between the three model predictions for Indonesian conditions. Thus, national design standards can be continuously refined to be more adaptive to the challenges of road conditions in Indonesia while aligning with developments in international methods.

CONCLUSION

The analysis results show that the structural response based on the 2024 Road Pavement Design Manual (MDPJ) analyzed with KENPAVE shows a systematic decreasing trend of strain in higher road classifications. *The maximum horizontal strain* decreased by 57% (from 0.0003238 to 0.0001392) and *the maximum vertical strain* decreased by 63% (from 0.0005397 to 0.0002003), proving the effectiveness of the 2024 Road Pavement Design Manual (MDPJ) in creating a stiffer structure for toll roads. This study also found that the Predicted Allowable Load Repetitions (ESAL) from the 2024 Road Pavement Design Manual (MDPJ) , Asphalt Institute , and AASHTO Mechanistic - Empirical Pavement Design consistently identified fatigue cracking *as a* critical failure

that occurs earlier than permanent deformation (*rutting*) in all road classifications. Based on the results of the analysis conducted, the ESAL values of fatigue cracking *for* road classification FFF (1) 2 are 3,054,833 ESAL (MDPJ 2024), 156,304 ESAL (Asphalt Institute), and 2,566,794 ESAL (AASHTO MEDDG). For FFF (1) 5, the ESAL values of fatigue cracking *are* 20,445,220 ESAL (MDPJ 2024), 588,082 ESAL (Asphalt Institute), and 15,822,112 ESAL (AASHTO MEDDG), respectively. At FFF (1) 7, the fatigue cracking ESAL values *obtained* were 66,851,081 ESAL (MDPJ 2024), 1,282,605 ESAL (Asphalt Institute), and 40,332,048 ESAL (AASHTO MEDDG). Meanwhile, for FFF (1) 9, the fatigue *cracking ESAL values* reached 139,231,482 ESAL (MDPJ 2024), 2,078,808 ESAL (Asphalt Institute), and 71,997,301 ESAL (AASHTO MEDDG). Although the resulting ESAL values were different, the dominant pattern of fatigue cracking *remained* the same.

REFERENCE

AASHTO. (2008). *Mechanistic-Empirical Pavement Design Guide* : A Manual of Practice. American Association of State Highway and Transportation Officials.

Almeida, A., Moreira, J. J. M., Silva, J. P., & Viteri, CG. V. (2021). Impact of traffic loads on flexible pavements considering Ecuador's traffic and pavement conditions. *International Journal of Pavement Engineering, 22* (6), 700–707. https://doi.org/10.1080/10298436.2019.1640362

Austroads. (2017). *Guide to pavement technology: Part 2 – Pavement structural design (AGPT02-17)* . Sydney, Australia: Austroads Ltd.

Banerjee, S., Manna, B., & Shahu, J. T. (2024). Experimental investigation of the geometry of geocells on the performance of flexible pavement under repeated loading. *Geotextiles and Geomembranes* , *52* (4), 654–670. https://doi.org/10.1016/j.geotexmem.2024.03.007

Bennert, T., Maher, A., & Gucunski, N. (2014). Calibration of MEPDG fatigue models for asphalt pavements. *International Journal of Pavement Engineering, 15* (2), 165–175. https://doi.org/10.1080/10298436.2012.748390

Ceylan, H., Schwartz, C. W., & Kim, S. (2009). Development of MEPDG permanent deformation models for subgrade soils. *Transportation Research Record, 2101* (1), 61–70. https://doi.org/10.3141/2101-07

Hadiwardoyo, SP, Sumabrata, RJ, & Berawi, MA (2012). TOLERANCE LIMIT FOR TRUCKS WITH EXCESS LOAD IN TRANSPORT REGULATION IN INDONESIA. *MAKARA of Technology Series* , *16* (1). https://doi.org/10.7454/mst.v16i1.1336

Hafeez, I., Kamal, M.A., Mirza, M.W., Barkatullah, & Bilal, S. (2013). Laboratory fatigue performance evaluation of different field laid asphalt mixtures. *Construction and Building Materials* , *44* , 792–797. https://doi.org/10.1016/j.conbuildmat.2013.03.083

Hussan, S., Kamal, M.A., Hafeez, I., Farooq, D., Ahmad, N., & Khanzada, S. (2019). Statistical evaluation of factors affecting the laboratory rutting susceptibility of asphalt mixtures. *International Journal of Pavement Engineering* , *20* (4), 402–416. https://doi.org/10.1080/10298436.2017.1299527

Jihanny, J. (2021). THE OVERLOAD IMPACT ON DESIGN LIFE OF FLEXIBLE PAVEMENT. *International Journal of GEOMATE* , *20* (78). https://doi.org/10.21660/2021.78.j2020

Ministry of Public Works and Public Housing. (2024). * *Road pavement design manual, No. 03/M/BM/2024* *. Jakarta: Directorate General of Highways.

Li, R., Schwartz, C. W., & Gibson, N. (2016). Probabilistic implementation of the MEPDG for flexible pavements. *Journal of Transportation Engineering, 142* (3), 04015065. https://doi.org/10.1061/(ASCE)TE.1943-5436.0000827

Rupiani, M., Subagio, BS, & Hariyadi, ES (2023). Comparative Analysis of Flexible Pavement Layer Thickness using *the MEPDG 2015 Method and the Asphalt Institute 1982 Method . Case study : Cirebon City – Losari Sub-district (Central Java Sub-district)* [Master's Thesis, Bandung Institute of Technology]. Digilib ITB. https://digilib.itb.ac.id/gdl/read/240782

Simanjuntak, I. (2014). Flexible Pavement Layer Thickness Evaluation Of Road Pavement Design Manual No.22.2/Kpts/Db/2012 Using The Kenpave Program.

Skrzypczak, I., Radwański, W., & Pytlowany, T. (2018). Durability vs technical—The usage properties of road pavements. *E3S Web of Conferences* , *45* , 00082. https://doi.org/10.1051/e3sconf/20184500082

The Asphalt Institute. (1982). *Thickness design—Asphalt pavements for highways and streets* (MS-1, 9 th ed.). The Asphalt Institute.

VenkatCharyulu, S., & Viswanadh, G. K. (2021). Flexible pavement design of district road. *E3S Web of Conferences* , *309* , 01210. https://doi.org/10.1051/e3sconf/202130901210

Wayne, M., Boudreau, R.L., & Kwon, J. (2011). Characterization of Mechanically Stabilized Layer by Resilient Modulus and Permanent Deformation Testing. *Transportation Research Record* : *Journal of the Transportation Research Board* , *2204* (1), 76–82. https://doi.org/10.3141/2204-10